Biosensors and Bioelectronics 135 (2019) 36–44

Contents lists available at ScienceDirect

Biosensors and Bioelectronics

journal homepage: www.elsevier.com/locate/bios

Electrochemical simultaneous analysis of dopamine and epinephrine using double imprinted One MoNomer acryloylated graphene oxide-carbon black composite polymer

Sana Fatma, Bhim Bali Prasad*, Swadha Jaiswal, Richa Singh, Kislay Singh

Analytical Division, Department of Chemistry, Institute of Science, Banaras Hindu University, Varanasi, 221005, India

ARTICLE INFO

Keywords:
Dual imprinting
Cross-linking monomer
Surface grafting from approach
Screen printed carbon electrode
Simultaneous analysis of neurotransmitters
Differential pulse anodic stripping voltammetry

ABSTRACT

A novel One MoNomer dual imprinted graphene oxide/carbon black composite polymer was developed applying 'surface-grafting from' approach on the screen printed carbon electrode for the electrochemical sensing of dopamine and epinephrine. Acryloylated-graphene oxide/carbon black was synthesized for the first time. This served both as a crosslinker and monomer leading to the fast electron transfer from the redox centre to the electrode. The oxidation peak potentials of both the targets were found separated by 200 mV which enabled their simultaneous analysis in real world samples, without any cross reactivity, interferences, and false-positives. The detection limits realized by the proposed sensor, under optimized analytical conditions, were found to be as low as 0.028, 0.028,0.061 and 0.029 ng mL^{-1} for dopamine and 0.017, 0.018, 0.019 and 0.020 ng mL^{-1} for epinephrine (S/N = 3) in aqueous, blood serum, urine and pharmaceutical samples. Such sensor could be considered suitable for the primitive diagnosis of several chronic diseases, manifested at ultra-trace level.

1. Introduction

Dopamine (DA) and epinephrine (EP) are important biological neurotransmitters ofcatecholamines class, present in mammals. These systems actively play vital roles in endocrine and central nervoussystemto stimulate the action of heart by increasingthe blood pressure. In fact, DA and EP are used together in the combined therapy for patients suffering from hypertension, bronchial asthma, and myocardial infarction. Since these targets are structurally similar and often coexist in biological samples [Cincotto et al., 2014; Ma et al., 2013; Figueiredo-Filhoet al.,2014], their electrochemical analysis is somewhat tedious due to overlapping of peaks.

Different methods such as capillary electrophoresis, high performance liquid chromatography-mass spectrometry, flow injection analysis with spectrophotometric detection and electrochemical studies are reported for DA and EP analyses [Wang and Chen, 2009; Li et al., 2007]. Electroanalytical methods have been relatively easy to determine DA and EP [Shankar et al., 2012; Zhang et al., 2009; Alothman et al., 2010; Huang et al., 2008; Santos et al., 2007; Choukairi et al., 2014; Ensafi et al., 2010; Yu et al., 2012; Goyal et al., 2008; Mazloum-Ardakani et al., 2010; Wang et al., 2006; Tavana et al., 2012; Shahrokhiana et al., 2009; Moghaddam et al., 2015; Yaghoubian et al., 2011; Sadeghi et al., 2013; Beitollahi et al., 2008; Mazloum-Ardakani et al., 2011; Ren et al., 2006] on individual basis. However, their estimation in combination was difficult when ascorbic acid (AA) and uric acid (UA) were present in the solution [Cincotto et al., 2014; Ma et al., 2013; Figueiredo-Filho et al., 2014].There have been some reports of simultaneous electrochemical determination of DA and EP [Cincotto et al., 2014; Ma et al., 2013; Figueiredo-Filho et al., 2014; Wang and Chen, 2009; Li et al., 2007; Chen and Peng, 2003; Zhang et al., 2013; Li 2010; Barman and Jasimuddin, 2016; Zhao et al., 2011]. However, these methods are not suitable for evaluation of chronic diseases manifested at ultra-trace levels. For instance, a new electrochemical device, silver nanoparticles-penicillamine-gold electrode, was recently introduced for the simultaneous determination of DA and EP, in the presence of AA and UA [Barman et al., 2016]. Nevertheless, this electrode was equivocal in terms of achieving sensitivity of the measurement beyond the presence of ten-fold excess interferents. The limits of quantitationof 0.17 and 0.09 ng mL^{-1}DA and EP, respectively, in blood plasma and serum are requisite [Ambade et al., 2009]. Thus, in order to attain high selectivity and such stringent level of sensitivity, one may procure molecularly imprinted polymer (MIP), in lieu of non-MIP systems.

MIPs are synthetic receptors prepared with the signature of template. It is imprinted in the presence of functional monomer, cross-linker, and initiator in a suitable medium called porogen. Particularly,

* Corresponding author.
E-mail address: prof.bbpd@yahoo.com (B.B. Prasad).

https://doi.org/10.1016/j.bios.2019.04.016
Received 11 February 2019; Received in revised form 2 April 2019; Accepted 8 April 2019
Available online 11 April 2019
0956-5663/

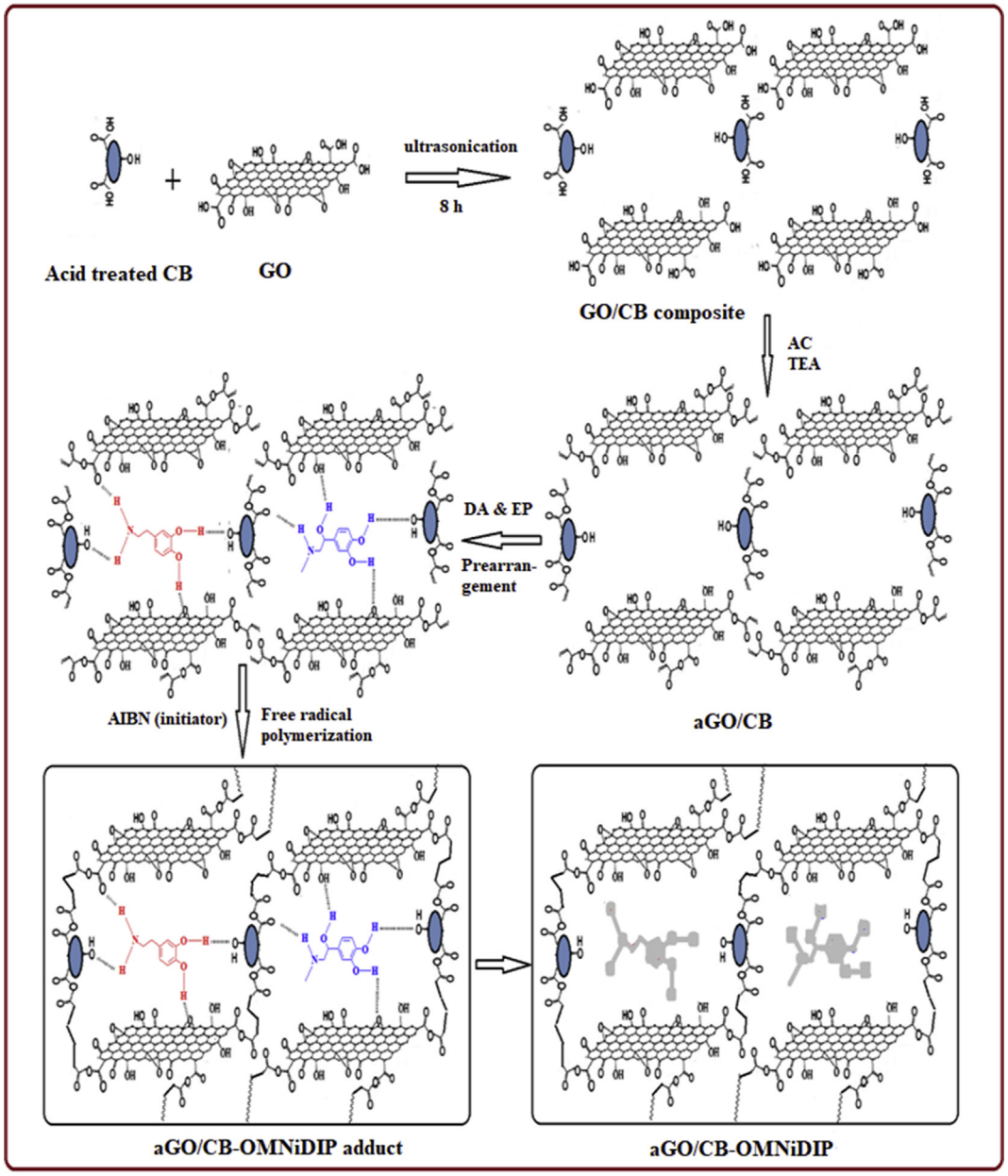

Scheme 1. Schematic protocol for the fabrication of aGO/CB-OMNiDIP.

multi-imprinting [Prasad and Jauhari,2015a; Prasad et al., 2014a; Prasad and Jauhari, 2015b; Prasad et al., 2014b; Prasad et al., 2017; Prasad et al., 2013a; Prasad and Fatma, 2017; Guo and Guo, 2013; Matsui et al., 2006]could be considered more attractive for the simultaneous analysis, since it saves both labor and time. However, one might encounter several chronic problems such as incomplete template retrieval, poor binding capacity, analyte diffusion constraint, and poor ingress-egress of analyte across the binding sites mostly located in the interior core. Alternatively, the surface imprinting technology could be considered more promising to resolve these problems [Li et al., 2018a; Liu et al., 2017; Li et al., 2018b]. Iron, gold, silica nanoparticles, carbon nanotubes (CNTs) and quantum dots etc., could be exploited as support for surface imprinting [Li et al., 2012]. Among other nanomaterials, graphene and its derivative graphene oxide (GO) have been reckoned as most promising candidates for application to develop MIP structures. These materials have specific electrochemical characteristics, such as high electrocatalytic activity, outstanding conductivity, high mobility of charge carriers, and rapid heterogeneous electron transfer [Lu et al., 2015]. One may incorporate carbon black (CB) into graphene layers to inhibit the agglomeration of GO and to improve electrolyte–electrode accessibility as well as electrode conductivity [Lu et al., 2015; Yan et al., 2010a; Yan et al., 2010b].

Simultaneous development of DA and EP, using dual imprinting, is not yet attempted. Notably, any use of cross-linker in traditional imprinting may hamper ingress-egress of the test analyte and reduce diffusion coefficient (*D*) [Prasad et al., 2016c]. As a remedy to this attendant problem, we propose a cage like polymer of acryloylated GO/CB (aGO/CB) monomer because it hasan excess of double bonds to produce a stable and homogenous system utilizing a cross-linking monomer. Such system is called as One MoNomer molecularly imprinted polymers (OMNiMIPs) [Prasad and Fatma, 2017; Prasad and Fatma, 2016; LeJeune and Spivak, 2009; Meng et al., 2009; LeJeune and Spivak, 2007; Spivak et al., 2005, LeJeune and Spivak, 2009; Fatma et al., 2019], where no external cross-linker is required.

2. Experimental

2.1. Reagents and apparatus

Reagents used in this work are detailed in the supporting data Section S1. Voltammetric measurements were made at 25 ± 1 °C, on a portable potentiostat μStat 200 (Drop Sens S.L. Oviedo, Spain). This unit was connected via USB connection to a computer installed with the measurement software Drop View (Drop Sens). Screen printed carbon electrode (SPCE) made of a ceramic substance was consisted of a working electrode (carbon, 4 mm diameter), a counter electrode (carbon) and a reference electrode (silver). Chronocoulometric measurementswere performed with the same electrode assembly using an electrochemical analyzer (CH instruments USA, model 1200 A). Fourier transforminfrared (FT-IR) spectra of GO, aGO/CB, aGO/CB-OMNiDIP-adduct, and aGO/CB-OMNiDIP were recorded on Varian 3100 FT-IR (USA) spectrometer using KBr thin pellets containing the sample. Surface morphologies of coatings were studied using scanning electron microscope (SEM), JEOL, JSM model-840 A and Atomic force microscope (AFM) (Vecco Instruments. Inc.,USA) with a nanoscope IIIa SPM controller (Digital Instruments, USA, tapping mode). Brunauer-Emmett-Teller (BET) analysis was made using a micromeritics ASAP 2020 apparatus at the temperature of liquid nitrogen −195.5 °C for obtaining surface area of the aGO/CB-OMNiDIP and its control system (aGO/CB-OMNiNIP). For the modification of SPCE surface with aGO/CB-OMNiDIP and aGO/CB-OMNiNIP, an indigenous spin-coater model SCU-2008 C (Apex Instruments, India) was used. Morphological study of GO/CB composite was made using tunnelling electron microscopy (TEM) [Technai-12FEI (Eindhoven, Netherlands)].

2.2. Synthesis of GO/CB composite

CB was firstly oxidized in a mixture of sulphuric acid and nitric acid (3:1) to yield -COOH group on its surface. GO was synthesized from natural graphite by the modified Hummers's method [Sun et al., 2011] [For details, vide supporting data Section S2]. The exfoliated GO/CB composite was prepared by 8 h ultrasonication of GO and CB (9:1, w/w) in 20.0 mL of water suspension and finally, the resultant solid was filtered, washed several times with waterand ethanol, and finally dried at 100 °C for 12 h in oven [Yan et al., 2010a].

2.3. Acryloylation of GO/CB

Acryloylated-GO/CB, a novel and crosslinking monomer, was first time synthesized as shown in Scheme 1. For this, acryloyl chloride (AC) was added dropwise into the suspension of GO/CB (0.05 g in 2.0 mL DMSO), in the presence of triethylamine (TEA) (1 mmol, 4.0 mL). A greyish black coloured product, acryloylated GO/CB croslinking monomer was obtained. The product was filtered and washed with NaOH-ethanol (5%, w/v) to remove untreated AC residue. [FT-IR (KBr) spectra max (cm^{-1}): 3540 (OH stretch), 1745 (C=O stretch of ester), 1706 (C=O stretch), 1657 (C=C vinyl stretch), 1620 (conjugated C=C stretch) (Fig. S1)].

2.4. Electrode fabrication

The working electrode in this work was SPCE, which was cleaned by sweeping potential between −0.5 and + 1.0 V in 0.5 M H_2SO_4 at scan rate 0.1 V s^{-1} [Vasilescu et al., 2003]. Thereafter, the electrode was covered with Teflon tape leaving exclusively the working electrode area free, for the synthesis of aGO/CB-OMNiDIP at the surface.

In this work, we have preferred the “surface-grafting from” approach for the coating of aGO/CB-OMNiDIP. For the preparation of aGO/CB-OMNiDIP-adduct/SPCE, solutions of templates (DA, 0.018 g in 250 μL dimethyl sulphoxide (DMSO)); EP, 0.018 g in 250 μL DMSO) and crosslinking monomer (aGO/CB, 0.036 g in 400 μL DMSO), were made separately. The crosslinking monomer was allowed to react with DA and EP solutions separately for half an hour. Latter, these solutions were thoroughly mixed. This helped self-assembling (pre-arrangement) of both the analytes with crosslinking monomer within a single matrix. Afterward, 0.02 mmol of an initiator, 2,2-azoisobutyronitrile, (0.003 g/100 μLDMSO) was added into it, followed by N_2 purging for 10 min. Thereafter, the resulting prepolymerization mixture (20 μL) was spin coated on to the surface of SPCE at 1500 rpm for 15 s. The firm coating of aGO/CB was due to the interaction of GO/CB (in the prepolymer mixture) with SPCE surface through the cumulative effect of physisorption and π- π interactions. This electrode was kept for 3.5 h in oven at 60 °C to initiate free radical polymerization on the interface to obtain aGO/CB-OMNiDIP-adduct/SPCE. After air drying, Teflon cover was removed from the modified SPCE. In order to generate imprinting cavities, template molecules were removed by stirring aGO/CB-OMNiDIP-adduct/SPCE into the TEA-Methanol solution (1:1, v:v) for 30 min. The complete template removal was ensured when no voltammetric response of the templates were noticed (vide Results and Discussion). The aGO/CB-OMNiDIP/SPCE so obtained was used as the working electrode for further studies. Similar method was adopted to prepare anon-imprinted polymer (NIP) modified electrode (aGO/CB-OMNiNIP/SPCE), in the absence of template molecules.

2.5. Electrochemical measurement

All voltammetric measurements were made in a cell containing 10.0 mL phosphate buffer solution (pH 7.2, 0.1 M) using aGO/CB-OMNiDIP/SPCE. The test solutions of both analytes were added into the cell after recording the blank run. The test analytes were allowed to accumulate at −0.6 V (accumulation potential, E_{acc}), for 210 s (accumulation time, t_{acc}), under dynamic condition followed by equilibration of 15 s. Deferential pulse anodic stripping voltammetry (DPASV) runs of analytes were recorded in the potential range varying from −0.3 to +1.0 V, at a scan rate 10 mVs^{-1}, pulse amplitude 25 mV, and pulse width 50 ms. Cyclic voltammetry (CV) experiments were performed in the potential window −0.5 to +0.8 V at various scan rates (20–200 mV s^{-1}) in anodic stripping mode. Since oxygen did not influence the voltammetry in the anodic potential window studied for the oxidative stripping of analyte, any deaeration of the cell content was not necessary. This was confirmed by recording DPASV runs, with and without nitrogen purging that revealed similar response in both conditions. The standard addition method was used to quantify all DPASVruns. For the calculation of the limit of detection (*LOD*, 3σ), three-fold standard deviation from the blank measurement (in the absence of templates) was taken which was divided by the slope of the calibration plot between analyte concentration and current.

3. Results and discussion

3.1. Material characteristics

Surface morphologies of aGO/CB-OMNiDIP/SPCE were examined with the help of SEM and AFM images.SEM image of aGO/CB-OMNiDIP/SPCE adduct shows a relatively compact structure due to intercalation of templates (small molecules) in the exfoliated space provided by two adjacent GO sheets supported on CB [Yan et al., 2010] (Fig. 1A). As such the structure of aGO/CB complex remained intact. However, on templates retrieval, the proposed sensor (aGO/CB-OMNiDIP/SPCE) surface revealed a porous structure with generation of molecular cavities of almost identical resemblance visible in Fig. 1B. The subsequent electrochemical measurements were governed by the porous structure of the film, possessing molecular cavities of DA and EP analytes. Side view of aGO/CB-OMNiDIP/SPCE (Fig. 1C) reveals the thickness of coating about 53.67 nm. The flakes of aGO/CB-OMNiDIP over SPCE are apparently adhered involving physical and π−π interactions. Fig. 1D presents a typical TEM image of GO/CB composite,

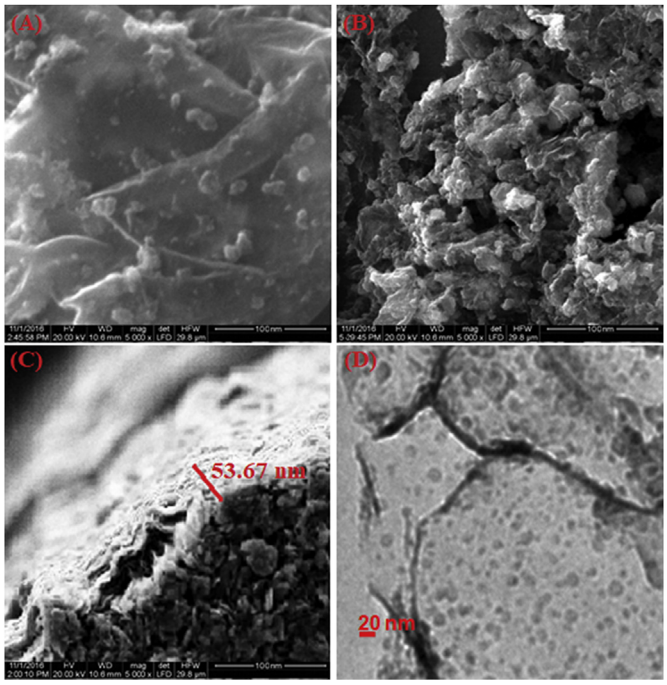

Fig. 1. SEM images: (A) aGO/CB-OMNiDIP-adduct/SPCE at 5000× magnification, and (B) aGO/CB-OMNiDIP/SPCE at 5000× magnification, and (C) side view of aGO/CB-OMNiDIP/SPCE at 5000× magnification showing film thickness; TEM image: (D) GO/CB composite.

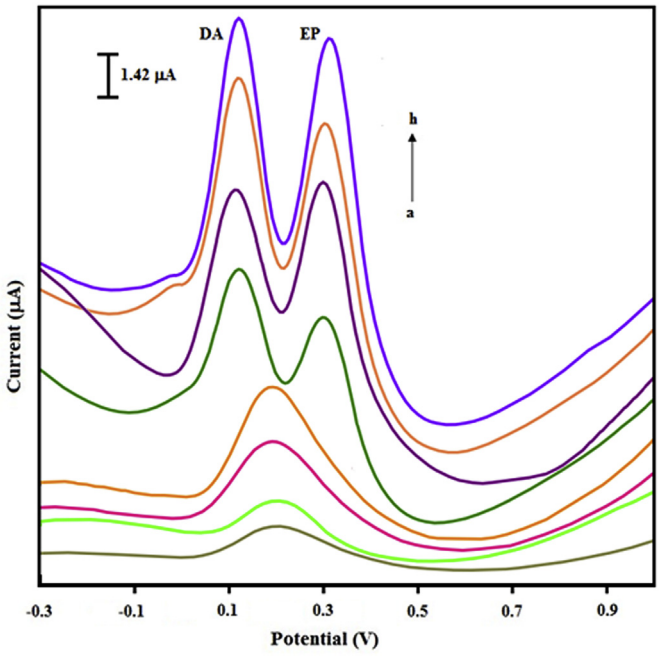

Fig. 2. DPASV response showing maximum currentwith DA (1.5 ng mL^{-1}) and EP (0.51 ng mL^{-1}) on different electrodes: (a) SPCE, (b) CB/SPCE, (c) GO/SPCE, (d) GO/CB composite/SPCE, (e) aCB-DIP/SPCE, (f) aGO-DIP/SPCE, (g) aGO/CB-DIP/SPCE, and (h) aGO/CB-OMNiDIP/SPCE. (Operating conditions: E_{acc} −0.6 V, t_{acc} 210 s, supporting electrolyte PBS (0.1 M, pH 7.2), pulse amplitude 25 mV, scan rate10 mV s^{-1}).

where all CB molecules are in contact to the exfoliated surface of GO, assuming spherical shapes (diameter10-20 nm). The larger exfoliation depends on the size of engrossed CB in between the layers of GO nanosheets [Yan et al., 2010a]. AFM images (Fig. S2) revealed 54.22 nm thickness of aGO/CB-OMNiDIP coating on exposed SPCE surface. This is in agreement with the data obtained by SEM images. [For details, vide supporting data Section S3, and Fig. S2 (A-B)].

FT-IR (KBr) spectra of GO, aGO/CB, templates (DA and EP), aGO/CB-OMNiDIP-adduct/SPCE, and aGO/CB-OMNiDIP/SPCE, were comparatively studied (Fig. S1) to support the proposed binding mechanism as shown in Scheme 1. The tentative image of cross-linking monomer (acryloylated CB in exfoliated acryloylated GO) after free radical polymerization in the presence of template(s) could apparently be assigned as a “cage” in the polymer backbone. The template(s)-cross-linking-monomer complexation involving hydrogen bond interactions are suggested on the basis of downward shift in IR bands of participating key groups of crosslinking-monomer and templates. It is pertinent that the proposed electrode showed no peak of templates after their removal from the adduct, reflecting the complete template retrieval process [For details, vide supporting data Section S4, Fig. S1].

Bare SPCE (Fig. 2, curve a) detects the presence of both the target analytes but fails to distinguish them due to overlapping potential. On modification with CB (Fig. 2, curve b) SPCE showed slight enhancement in current. This peak was found to be increased more when SPCE was modified with only GO (Fig. 2, curve c) due to channelizing electron transport from electrolyte to electrode surface. On the other hand, the composite GO/CB coated SPCE current (Fig. 2, curve d) was considerably improved drastically due to the prevalent hetro-junctions present between GO and CB that enabled an enhanced electron transfer rate [Prasad and Fatma, 2017]. But problem is yet to be resolved with GO/CB composite in separation of peaks of both the target molecules. This shortcoming was overcome, however, using traditional molecular imprinting technique. When acryloylated CB based double imprinted polymer sensor, was used, the well resolved simultaneous responses of DA and EP were observed. It may be noted that aGO-DIP/SPCE (Fig. 2, curve f) responded better than aCB-DIP/SPCE, apparently due to better conductivity of GO as compared to CB. Nevertheless, in view of the probable hetro-junctions in GO-CB composite which enhance the current response, aGO/CB-DIP/SPCE (Fig. 2, curve g) was found to have improved resolution as well as the conductivity of the sensor. Notably, traditional imprinting involving monomer and crosslinker (EGDMA) which yield curves e, f and g, can be enhanced to a larger extent when external cross-linker system (EGDMA) is avoided in the polymerization process. As a matter of fact, the external crosslinker blocks cavities resulting in reduced porosity of the film. Therefore, in this work aGO/CB-OMNiDIP/SPCE (Fig. 2, curve h) was fabricated which not only showed complete resolution but also yielded an approximately 2-fold higher response than aGO/CB-DIP/SPCE. Herein, aGO/CB has excessive double bonds to behave as excellent cross-linking monomer and therefore relegate the use of any external cross-linker.

Maximum development of current response was ensured by-optimizing the polymerization conditions such as polymerization time (3.5h), polymerization temperature (60 °C), and template:template:-cross-linking monomer ratio (w/w) (1:1:2). [For details, vide supporting data Section S5 and Fig. S3]. Specific surface areas for aGO/CB-OMNiDIP and aGO/CB-OMNiNIP were calculated to be 210.2 $m^2 g^{-1}$ and 131.2 $m^2 g^{-1}$, respectively. [For details, vide supporting data Section S6].

The graft efficiency (E_g, mol cm^{-2}) was obtained using following equation:

$$Eg = (Vb - Vs)C/2A \quad [1]$$

where *Vb* and *Vs*, are the volumes of $Na_2S_2O_3$ standard solutionconsumed in the blank and sample experiments (in the absence and presence of electrode), respectively; *C* is the concentration of $Na_2S_2O_3$ standard solution (mol L^{-1}), and *A* is the area of bare SPCE (cm^2). The values of E_g obtained with different electrodes using varying amount of aGO/CB are shown in Fig. S4. The spin-coating of varying amount (0.018, 0.036, 0.054, 0.072 g per 400 µL DMSO) of aGO/CB (15 µL) suspension on the surface of SPCE along with subsequent modification with aGO/CB-OMNiDIP showed interesting results. The maximum

development of DPASV current for both the analyte [2.00 ng mL^{-1} (DA) and 0.56 ng mL^{-1} (EP)] was observed when the aGO/CB-OM-NiDIP/SPCE was made with 0.036 g monomer suspension in 400 µL DMSO to reveal graft efficiencyof 98.0 mmol/cm^2 [For details, see Supporting Information S7 and Fig. S4].

3.2. Electrochemical studies

For electrochemical studies, all operating conditions such as accumulation potential (E_{acc} = −0.6), accumulation time (t_{acc} = 210 s), and pH (7.2) of the test solution were optimized for the maximum development of DPASV response at scan rate 10 mV s^{-1}for DA (1.20 ng mL^{-1}) and EP (0.40 ng mL^{-1}), using aGO/CB-OMNiDIP/SPCE [For details on optimization of experimental conditions, vide Supporting Information S8 and Fig. S5]. In this study, both templates were first accumulated simultaneously over aGO/CB-OMNiDIP/SPCE at −0.6 V (*vs.* Ag/AgCl) for 210 s, in their respective cavities. Entrapped analytes were then allowed to anodically strip off after 15 s equilibration. As a result, a pseudo-reversible CV peak (I) for DA (0.39 ng mL^{-1}), with potential separation ($\Delta E_p = E_{pa}$-E_{pc}) of 0.150 V, and an irreversible CV peak (II) for EP (0.12 ng mL^{-1}) were obtained at scan rate 100 mV s^{-1} on aGO/CB-OMNiDIP/SPCE in the phosphate buffer (0.1 M), pH = 7.2 (Fig.S6). The electron-transfer processes for DA followed 2e$^-$, 2H$^+$ mechanism as reported elsewhere [Prasad et al., 2013a]. CV peak for EP is based on the known irreversible oxidation (2e$^-$, 2H$^+$) mechanism [Prasad et al., 2013b]. Interestingly, these analytes retained their diffusion-controlled characteristics, even when analyzed simultaneously. This couldbe evinced by following linear relationships.

- [2]

DA :$Ipa = (68.846 \pm 5.749)\nu^{1/2} + (-8.166 \pm 1.749)\,(R^2 = 0.99)$

$Ipc = (49.110 \pm 0.638)\nu^{1/2} + (-6.154 \pm 0.194)\,(R^2 = 0.99)$ [3]

- [4]

EP :$Ipa = (76.792 \pm 8.939)\nu^{1/2} + (-9.795 \pm 2.718)\,(R^2 = 0.97)$

The observed positive shift of both peaks with increasing scan rate may be accorded with the difficulty in stripping process in short duration, and thus required a higher energy for the oxidation.

The number of electrons (n = 1.8 and 1.9), diffusion coefficient (D = 0.78 x 10^{-4}and 1.23 x 10^{-4} cm^2 s^{-1}), and total surface coverage (I° = 1.13 x 10^{-10} and 2.36 x 10^{-10} mol cm^{-2}) for DA and EP, respectively were obtained chronocoulometrically in a separate experiment. Multiplying the surface coverage (I°) with effective surface area [(2.54 cm^2) by applying Randles Sevcik equation [Bard and Faulker, 2001] using ferricyanide probe on modified electrode] revealed that as many as 17.29 x 10^{13} molecules of DA and 36.10 x 10^{13} molecules of EP were bound in their respective cavities. Chronocoulometric studies also revealed that the proposed sensor showed much higher D values (15–16 times) for both analytes as compared to aGO/CB-DIP/SPCE (Table S1) [For details, vide supporting data Section S9].

The following equation was used to determine the electron-transfer rate constant (k) for DA on the modified electrode ($n\Delta Ep \geq 200$ mV, $\Delta E_p = E_{pa}$-E_{pc}) [Laviron, 1979]:

$$\log k = \alpha \log(1-\alpha) + (1-\alpha)\log\alpha - \log\frac{RT}{nF\nu} - \frac{\alpha(1-\alpha)nF\Delta E_p}{2.3RT} \quad [5]$$

where α is the electron-transfer coefficient, F is the Faraday constant, ν the scan rate (V s^{-1}), R the gas constant, T the temperature, and n is the number of electrons. The α value 0.69 for DA could be obtained from the slope (2.303RT/(1- α)nF) of E_p vs. log ν plot. Substituting α value in Eq. (5) revealed k value for DA to be 13.04 x 10^{-2} s^{-1}. The fractional α value suggests electron transfer process in DA oxidation to be quasireversible. Insofar as the k value for the irreversible oxidation of the stripped EP molecules (n = 2) is concerned, we have applied CV data in the following equations reported for irreversible electron-transfer reactions [Meites, 1965]:

$$\alpha n = 1.857\frac{RT}{F}(E_{pa} - E_{pa/2}) \quad [6]$$

$$E_{pa} = E_{pa/2} - b\left[0.52 - 0.5\log\frac{b}{D} - \log k_s + 0.5\log\nu\right] \quad [7]$$

$$b = \frac{2.303RT}{\alpha nF} \quad [8]$$

where b is Tafel coefficient, α is electron transfer coefficient (0.298), and other parameters have their usual meanings. Accordingly, the heterogeneous electron transfer rate constant (k) of the irreversible EP oxidation is obtained to be 15.04 x 10^{-2} s^{-1}.

Further, the simultaneous adsorption of both analytes in structurally cage like polymer was followed in accordance with the Langmuir linear adsorption model. Other adsorption isotherms such as Freundlich and Scatchard were not suited in the present instant as these are known to be good for multilayer adsorption with sufficient conflict of interaction between absorbing molecules. The adsorption coefficients (B_{ads}) were found to be 7.72 × 10^{7}and 2.82 × 10^7 Lmol^{-1} for DA and EP, respectively. For adsorption of analytes, the Gibbs free energy changes (ΔG_{ads} = -RT ln B_{ads}) were found to be −45 kJ mol^{-1} for DA and −42.5 kJ mol^{-1} for EP. This indicated that the spontaneous adsorption for both analytes was realized without any conflict of interactions [For details, vide supporting data Section S10].

3.3. Aqueous and real sample analysis

The aGO/CB-OMNiDIP/SPCE sensor was used for the simultaneous analysis of DA and EP in aqueous as well as real samples. For this, DPASV technique was preferred to CV because of negligible background current associated with DPASV measurements in the sufficient time scale (pulse amplitude 25 mV, pulse width 50 ms) of voltammetry. DPASV curves for individual analyte on proposed sensor are illustrated in Fig. S7. Adsorptive behaviour of both analytes and their mutual effect were studied at length [Prasad and Jauhari, 2015a]. For this DA was deliberately kept at a fixed concentration (1.92 ngmL^{-1}) and EP concentration was varied from 0.079 to 1.307 ng mL^{-1}[Fig. 3A (curves b-j)]. Accordingly, a linear calibration plot (Fig. 3D) between current (I_p, µA) and concentration (ng mL^{-1}) was obtained. In the similar way, EP concentration was kept constant (1.320 ng mL^{-1}) and DA was varied from 0.115 to 5.909 ng mL^{-1} [Fig. 3B (curves b-g)] to lead a linear regression curve (Fig. 3E). Nevertheless, one may obtain symmetrical DPASV peaks for both analytes simultaneously at their oxidation potentials. In this case, DA concentration varied from 0.120 to 4.578 ng mL^{-1} and EP concentration varied from 0.075 to 1.188 ng mL^{-1} [Fig. 3C, (curves b-i)]. The calibration equations for simultaneous DA and EP were also found to be linear (Fig. 3F) in the wide range of concentrations. Curve “a” in all figures (Fig. 3A–C) represent the blank response with the proposed sensor. Since this curve did not respond any peak due to DA and EP, the complete retrieval of template(s) could be feasible as supported by respective FT-IR studies (Fig. S1).

Since simultaneous peaks for DA and EP appeared at their respective positions similar to individuals (Fig.S7), the electrode processes for both analytes in the present study could be considered to occur independently, on the double imprinted electrode surface. The aGO/CB-OMNiDIP/SPCE was tested for the selective and sensitive analysis of DA and EP in real samples containing test analyte in biological (blood serum and urine) samples (Fig.S8) and pharmaceutical formulations (Fig. S9). Fig. S8 did not reveal any peak in blank runs (curve “a”) which supported the complete removal of DA and EP after template extraction. Interestingly, when mixture of interferents was exclusively

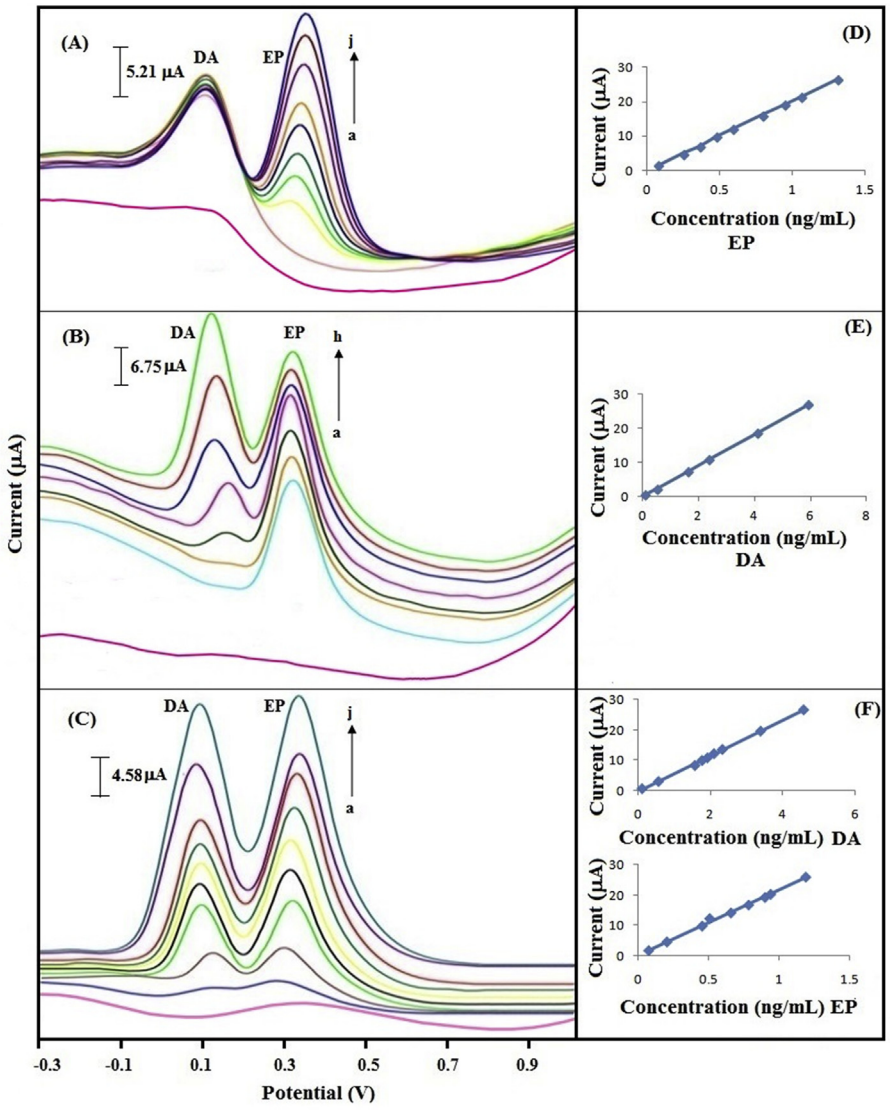

Fig. 3. (A) DPASV runs of different concentration of EP at aGO/CB-OMNiDIP/SPCE in the presence of fixed concentration (1.92 ng mL^{-1}) of DA, [b to j (0.079–1.307 ng mL^{-1})]; (B) DPASV runs of different concentration DA at aGO/CB-OMNiDIP/SPCE in the presence of fixed concentration (1.32 ng mL^{-1}) of EP, [b to h (0.115–5.909 ng mL^{-1})]; (C) DPASV runs obtained for the simultaneous analysis of EP and DA at aGO/CB-OMNiDIP/SPCE, [DA concentration varied from b to j (0.120–4.578 ng mL^{-1}) and EP concentration varied from a to k (0.075–1.188 ng mL^{-1})]; curve 'a' in Fig (A), (B), and (C) areblank control curve, which are obtained in the detection solution without any analyte using aGO/CB-OMNiDIP/SPCE; Fig (D), (E) and (F) are the linear calibration curves corresponding to Fig. (A), (B) and (C), respectively. (Operating conditions: same as with Fig. 2).

present in phosphate buffer (no DA and EP), the proposed sensor was not at all DPASV responsive for the interferents. This was also true with biological samples responding the endogenous concentration of DA and EP and with pharmaceutics responding only DA and EP; no interferent response was noticed in real samples. Despite the identical structures of some of the interferents like norepinephrine, the proposed sensor was substrate-specific, for the print molecules (targets) owing to phenomenal imprinting effect [imprinting factor19.0 (DA) and 59.3 (EP)]. All analytical results are summarized in Table 1, depicting linear regression equation, range, recovery, limit of detection (*LOD*), etc. Beyond the observed linear concentration ranges, DPASV currents were found to be constant owing to the binding sites saturation. This necessitated blood serum and urine samples to be diluted 2.0 and 187.6 folds, respectively so as to move the detection in the sensing range of the electrode.The best part of this work is that any pre-treatment (i.e, ultra-filtration, centrifugation, and deproteinization) of biological fluids was deliberately avoided sincethis may lead inaccuracy to the final results as far as ultra-trace analysis is concerned. Table 1 portrays excellent analytical figure of merits (i.e, precision, selectivity, sensitivity, etc). Interestingly, when samples contained either of the analytes alone or consisted both DA and EP together, slopes (sensitivities) of respective linear calibration equations for DA were found slightly different from those for EP. This indicated reproducibility of voltammetric measurements, giving slightly varied sensitivity and diffusion kinetics. Also, the sample dilutions carried out in this work did not affect the measurement sensitivity but rather advantageous to obviate the effect of complicated matrices. A close perusal of Table 1 revealed that all real samples, upon massive dilutions, had assumed their sample behaviour (slope, range, *LOD*) very close to the aqueous samples. In nutshell, the devised sensor is capable to analyse the simultaneous mixture of pair of analytes at their stringent ultra-trace limits in real samples, without any cross-reactivity and matrix effect. The proposed sensor is validated comparing a known method [4] by means of student's t-test [DA: $t_{cal}(2.21) < t_{tab}(4.30)$, EP: $t_{cal}(2.61) < t_{tab}(4.30)$]. In this context,it is also worth to compare the present work with other known sensors, reported in the past decade (Table S2).

Notably, none of above work reported earlier was MIP-based and thus selectivities in these works were jeopardized. These could be considered inferior in judging the low levels or complete depletion of DA and EP in the central nervous system to cause several neurological disorders like Parkinson's disease, Schizophrenia, Huntington's disease, HIV, drug addiction, hypertension, bronchial asthma, cardiac surgery, and myocardial infection, etc. Several work reported earlier were not comprehensively done with real sample analysis and moreover, diffusion coefficient, surface area, total surface coverage and heterogeneous electron transfer, etc. were not adequately obtained. The sensor

Table 1
Analytical results of DPASV measurements on aGO/CB-OMNiDIP/SPCE in aqueous and real samples.

Sample	Analyte(s)	Regression equation	Linear range (ng mL^{-1})	Recovery[a] (%)	*LOD*[b] (ng mL^{-1})	*RSD*[c] (%) (for three sets of *LODs*)	Endogenous concentration[d] (ng mL^{-1})
Aqueous	DA (individual)	$I_p = (5.962 \pm 0.001)\,C + (0.012 \pm 0.014)$, $n = 8$, $R^2 = 0.99$	0.116–6.231	97.5–104.3	0.026	0.31	–
	EP (individual)	$I_p = (22.203 \pm 0.001)C + (-0.001 \pm 0.010)$, $n = 9$, $R^2 = 0.99$	0.074–1.832	95.5–104.8	0.017	0.26	
	DA (with 1.32 ng mL^{-1} EP; fixed)	$I_p = (4.577 \pm 0.005)\,C + (0.02 \pm 0.018)$, $n = 6$, $R^2 = 0.99$	0.115–5.909	98.8–101.6	0.026	0.16	
	EP (with 1.92 ng mL^{-1}DA; fixed)	$I_p = (20.360 \pm 0.151)\,C + (0.004 \pm 0.114)$, $n = 9$, $R^2 = 0.99$	0.079–1.307	98.0–105.0	0.018	0.36	
		$I_p = (5.867 \pm 0.075)\,C + (0.389 \pm 0.334)$, $n = 9$, $R^2 = 0.99$	0.12–4.578	98.1–103.3	0.028	0.15	
	DA and EP mixture	$I_p = (21.277 \pm 0.462)\,C + (0.289 \pm 0.334)$, $n = 9$, $R^2 = 0.99$	0.075–1.188	98.5–103.5	0.017	0.23	
Blood serum (diluted-2 fold)	DA	$I_p = (5.410 \pm 0.055)C + (0.186 \pm 0.161)$, $n = 7$, $R^2 = 0.99$	0.122–4.783	97.2–102.5	0.028	0.35	0.244
	EP	$I_p = (17.803 \pm 0.0816)C + (0.035 \pm 0.077)$, $n = 7$, $R^2 = 0.99$	0.079–4.436	99.1–104.3	0.018	0.38	0.158
Urine (diluted-187.6)	DA	$I_p = (5.269 \pm 0.041)C + (0.207 \pm 0.118)$, $n = 6$, $R^2 = 0.99$	0.277–4.519	98.2–103.7	0.061	0.37	52.003
	EP	$I_p = (17.876 \pm 0.047)C + (0.081 \pm 0.041)$, $n = 6$, $R^2 = 0.99$	0.08–1.479	99.4–101.9	0.019	0.29	15.008
Pharmaceutical (DA (diluted-3.19 x 10^7)	DA	$I_p = (5.152 \pm 0.011)C + (0.104 \pm 0.014)$, $n = 7$, $R^2 = 0.99$	0.125–4.620	98.2–101.8	0.029	0.23	3.99 x 10^7 (certified value 4 x 10^7)
(EP diluted-1.25 x 10^6 fold)	EP	$I_p = (18.522 \pm 0.021)C + (0.74 \pm 0.017)$, $n = 7$, $R^2 = 0.99$	0.08–1.413	97.5–103.2	0.020	0.37	10.02 x 10^4 (certified value 10 x 10^4)

[a] % Recovery = (amount of analyte determined/amount of analyte taken) x 100.
[b] *LOD* based on the minimum distinguishable signal for lower concentrations of analyte (*S/N* = 3, 95% confidence level).
[c] *RSD* (%) for three sets of *LOD* data.
[d] Endogenous concentration is the original concentration of analyte obtained by the multiplication of the extreme lower concentration data with the respective dilution factor.

reported in this work is quite practical, without any cross-reactivity and false positives, for simultaneous analysis of DA and EP in real world samples.

3.4. Interferences

As many as twelve clinically viable interferents, viz., ascorbic acid (AA), uric acid (UA), norepinephrine (NE), L-tyrosine (Tyr), L-tryptophan (Trp), creatinine (Crea), creatine (Cre), serotonine (Ser), glycine (Gly), glutamic acid (Glu), glucose (Glc), urea, and their mixture were studied to explore theinterference in this work (Table S3). Interestingly, the non-imprinted (aGO/CB-OMNiNIP-modified) electrode had casted some interferences in individual capacity (Fig. 4). Such interferences were, however, removed simply by water washings (n = 3.0, 1.0 mL). This necessitates the similar washing treatments to obviate any false positive with the proposed sensor [Prasad et al., 2016]. A parallel study with the mixtures of templates and interferent(s), concomitantly present with samples in the clinically relevant concentration ratios, was also explored. As evident from Fig. 4, aGO/CB-OMNiDIP/PGE showed quantitative (100%) adsorption of DA and EP, without any cross-reactivity between them and without having any effect of interferents. As a matter of fact, the real samples had also shown no cross-reactivity between DA and EP and yielded the quantitative response on aGO/CB-OMNiDIP/SPCE (Fig. S7).

When either analyte or interferent (each 0.2 ng mL^{-1}) were studied individually, without undergoing any water-washing treatment after their adsorptions, with aGO/CB- OMNiDIP/SPCE and the corresponding aGO/CB-OMNiNIP/SPCE, the selectivity coefficient (k) and relative selective coefficient (k') were obtainedfor both the templates with respect to interferents/structural analogues (Table S3). Almost no interference ($k' < 6.3\%$ for DA and $k' < 2.2\%$ for EP) was observed with any of the interferents studied. The reason could be based on the fact that the interferent(s), like NE (structurally similar to DA and EP), Crea, Cre, Gly, Glu, and Urea (smaller in size than DA and EP), have a fair chance of approaching the imprinting sites but still mismatch the imprinting sites in terms of chemical affinity and size. The extremely poor relative k and k' values for all interferents indicated simultaneous analyte selectivity in cavities. For this, the due credit be given to the successful dual imprinting in a single structurally cage like polymeric network. As a matter of fact, the present sensor has shown the imprinting factors (α) as high as19.0 and 59.3 for DA and EP, respectively. [For endurance and precision of proposed sensor vide supporting data Section S11].

4. Conclusion

For the first time, aGO/CB composite based One MoNomer dual imprinted polymer having “cage” structure was developed over the surface of SPCE, to analyse DA and EP, simultaneously, in aqueous/real samples. Herein, aGO/CB served both as a crosslinking monomer for the fast electron transfer from the redox centre to the electrode. The highly exfoliated nanostructured aGO/CB-OMNiDIP was advantageous to obtain a sensory platform with larger surface area and a very thin film of about 53.67 nm for the faster ingress and egress of analytes. This led to the successful determination of both DA and EP at stringent limits in both biological and pharmaceutical samples, without any cross-reactivity, false positives (non-specific), and matrix effect. The limits of quantitation (S/N = 10) of DA and EP were realized in this work to be as low as 0.115 and 0.075 ng mL^{-1}, respectively. However, the limits of detection (S/N = 3) were very precised in the range of 0.028–0.061 ng mL^{-1} for DA and 0.017–0.020 ng mL^{-1} for EP in aqueous/real samples.The corresponding imprinting factors were as high as 19.0 and 59.3 for DA and EP, respectively, in all samples studied. The ultra high sensitivity of the proposed sensor is attributed to the higher electron transfer rate constants (k = 13.04 x 10^{-2} s^{-1} and15.04 x 10^{-2} s^{-1} for DA and EP, respectively). The proposed sensor could be practically viable in clinical setting for simultaneous evaluation of DA and

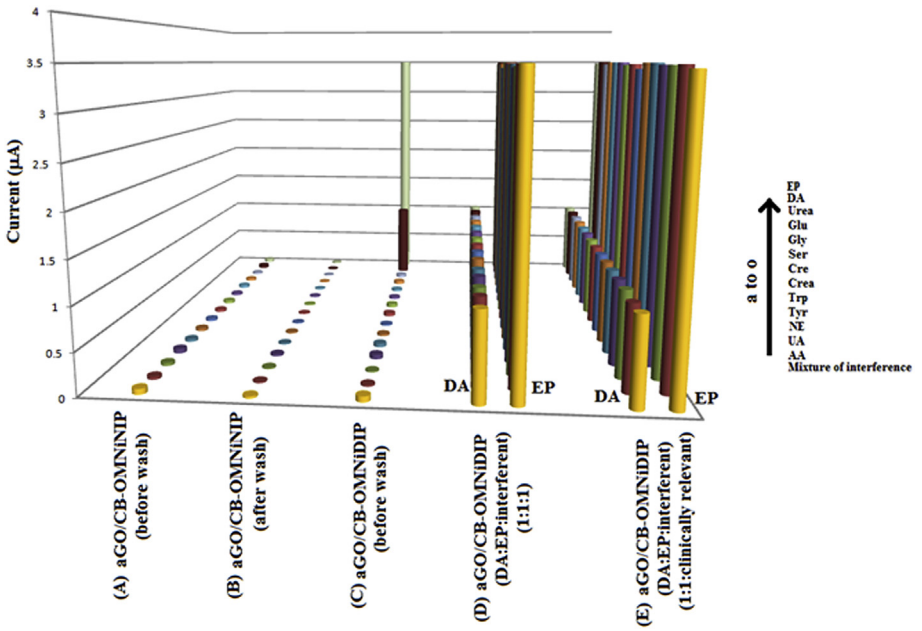

Fig. 4. DPASV response at modified SPCEs when both the templates and interferent(s) (each 0.2 ng mL^{-1}) measured individually on aGO/CB-OMNiDIP/SPCE: (A) before water washing and (B) after water washing; (C) when measured individually on OMNiDID/PGE. OMNiDID/PGE response when DA and EP measured in the mixture with interferent (s) (1:1:1) (concentration 0.2 ng mL^{-1}) (D) and when DA and EP (each 0.43 ng mL^{-1}) are measured with interferences taken in their respective clinical concentrations [2000 (AA), 2000 (UA), 0.2 (NE) 2000 (Tyr), 2000 (Trp), 2000 (Crea), 2000 (Cre), 200 (Ser), 20000 (Gly), 2000 (Glu), 20000 (Glc), 200000 ng mL^{-1}Urea, and mixture of interferents] (E). (Operating conditions: same as with Fig. 2).

EP, in wide concentration ranges (Table 1).

Declaration of interests

The authors declare that they have no known competing financial interests or personal relationships that could have appeared to influence the work reported in this paper.

CRediT authorship contribution statement

Sana Fatma: Conceptualization, Data curation, Formal analysis, Funding acquisition, Investigation, Methodology, Project administration, Resources, Software, Validation, Visualization, Writing - original draft, Writing - review & editing. **Bhim Bali Prasad:** Supervision, Project administration, Resources, Visualization, Writing - original draft. **Swadha Jaiswal:** Writing - review & editing. **Richa Singh:** Data curation, Validation. **Kislay Singh:** Writing - review & editing.

Acknowledgements

Authors thank University grant commission, New Delhi for research fellowship to S.F, S.J. and CSIR-SRF fellowship to K.S. Instrumental facilities procured from B.H.U. are also greatly acknowledged.

Appendix A. Supplementary data

Supplementary data related to this article can be found at https://doi.org/10.1016/j.bios.2019.04.016.

References

Alothman, Z.A., Bukharia, N., Wabaidur, S.M., Haider, S., 2010. Sensor. Actuator. B Chem. 146, 314–320.
Ambade, V., Arora, M.M., Singh, P., Somani, B.L., Basannar, D., 2009. J. Armed Force India 65, 216–220.
Barman, K., Jasimuddin, S., 2016. RSC Adv. 6, 99983–99988.
Bard, A.J., Faulker, L.R., 2001. Electrochemical Methods, second ed. Wiley, New York.
Beitollahi, H., Karimi-Maleh, H., Khabazzadeh, H., 2008. Anal. Chem. 80, 9848–9851.
Chen, S.-M., Peng, K.-T., 2003. J. Electroanal. Chem. 547, 179–189.
Choukairi, M., Bouchta, D., Elbouhouti, H., de Cisneros, J.L.H.H., Rodriguez, I.N., 2014. IJIRSET 3, 11159–11166.
Cincotto, F.H., Canevari, T.C., Campos, A.M., Landers, R., Machado, S.A.S., 2014. Analyst 139, 4634–4640.
Ensafi, A.A., Dadkhah-Tehrani, S., Rezaei, B., 2010. J. Serb. Chem. Soc. 75, 1685–1699.
Fatma, S., Prasad, B.B., Singh, K., Singh, R., Jaiswal, S., 2019. Sensor. Actuator. B Chem. 281, 139–149.
Figueiredo-Filho, L.C.S., Silva, T.A., Vicentini, F.C., Fatibello-Filho, O., 2014. Analyst 139, 2842–2849.
Goyal, R.N., Gupta, V.K., Bachheti, N., Sharma, R.A., 2008. Electroanalysis 20, 757–764.
Guo, Y., Guo, T., 2013. Chem. Commun. 49, 1073–1075.
Huang, J., Liu, Y., Hou, H., You, T., 2008. Biosens. Bioelectron. 24, 632–637.
Laviron, E., 1979. J. Electroanal. Chem. 101, 19–28.
LeJeune, J., Spivak, D.A., 2007. Anal. Bioanal. Chem. 389, 433–440.
LeJeune, J., Spivak, D.A., 2009. Biosens. Bioelectron. 25, 604–608.
Li, N.B., Ren, W., Luo, H.Q., 2007. Electroanalysis 19, 1496–1502.
Li, X., 2010. Int. J. Chem. 2, 206–211.
Li, Y., Li, Y., Zhu, E., McLouth, T., Chiu, C.-Y., Huang, X., Huang, Y., 2012. J. Am. Chem. Soc. 134, 12326–12329.
Li, Y., Liu, J., Zhang, Y., Gu, M., Wang, D., Dang, Y.Y., Ye, B.C., Li, Y., 2018a. Biosens. Bioelectron. 106, 71–77.
Li, Y., Zhang, L., Dang, Y., Chen, Z., Zhang, R., Li, Y., Ye, B.C., 2018b. Biosens. Bioelectron. 127, 207–214.
Liu, J., Zhang, Y., Jiang, M., Tian, L., Sun, S., Zhao, N., Zhao, F., Li, Y., 2017. Biosens. Bioelectron. 91, 714–720.
Lu, L., Zhang, F., Xia, J., Wang, Z., Liu, X., Yuan, Y., 2015. Int. J. Electrochem. Sci. 10, 1646–1657.
Ma, W., Yao, X., Sun, D., 2013. Asian J. Chem. 25, 6625–6634.
Matsui, J., Sodeyama, T., Tamaki, K., Sugimoto, N., 2006. Chem. Commun. 0, 3217–3219.
Mazloum-Ardakani, M., Beitollahi, H., Amini, M.K., Mirkhalaf, F., Abdollahi-Alibeika, M., 2011. Anal. Methods 3, 673–677.
Mazloum-Ardakani, M., Rajabi, H., Beitollahi, H., Mirjalili, B.B.F., Akbari, A., Taghavinia, N., 2010. Int. J. Electrochem. Sci. 5, 147–157.
Meites, L., 1965. Polarographic Techniques, second ed. Willey Intersciences, New York.
Meng, A.C., LeJeune, J., Spivak, D.A., 2009. J. Mol. Recognit. 22, 121–128.
Moghaddam, H.M., Beitollahi, H., Tajik, S., Soltani, H., 2015. Electroanalysis 27, 2620–2628.
Prasad, B.B., Fatma, S., 2016. Sens Actuators B:Chem. 229, 655–663.
Prasad, B.B., Fatma, S., 2017. Electrochim. Acta 232, 472–483.
Prasad, B.B., Jaiswal, S., Singh, K., 2017. Sens Actuators B:Chem. 240, 631–639.
Prasad, B.B., Jauhari, D., 2015a. Anal. Chim. Acta 875, 83–91.
Prasad, B.B., Jauhari, D., 2015b. Sens Actuators B:Chem. 207, 542–551.
Prasad, B.B., Jauhari, D., Tiwari, M.P., 2013a. Biosens. Bioelectron. 50, 19–27.
Prasad, B.B., Jauhari, D., Tiwari, M.P., 2014b. Biosens. Bioelectron. 59, 81–88.
Prasad, B.B., Jauhari, D., Verma, A., 2014a. Talanta120. pp. 398–407.
Prasad, B.B., Prasad, A., Tiwari, M.P., Madhuri, R., 2013b. Biosens. Bioelectron. 45, 114–122.
Prasad, B.B., Singh, R., Kumar, A., 2016. Carbon 102, 86–96.
Ren, W., Luo, H.Q., Li, N.B., 2006. Sensors 6, 80–89.
Santos, P.M., Sandrino, B., Moreira, T.F., Vishwanatha, C.C., Swamy, B.E.K., Pai, K.V., 2015. J. Anal. Bioanal. Tech. 2, 1–5.
Sadeghi, R., Karimi-Maleh, H., Bahari, A., Taghavi, M., 2013. Phys. Chem. Liq. 51, 704–714.
Shahrokhiana, S., Ghalkhani, M., Amini, M.K., 2009. Sens Actuators B:Chem. 137, 669–675.
Shankar, S.S., Swamy, B.E.K., Chandrashekar, B.N., 2012. J. Mol. Liq. 168, 80–86.
Spivak, D.A., Sibrian-Vazquez, M., Houck, S., 2005. Polym. Preprint. 46, 1103–1104.
Sun, H., Yang, Y., Huang, Q., 2011. Integr. Ferroelectr. 128, 163–170.

Tavana, T., Khalilzadeh, M.A., Karimi-Maleh, H., Ensafi, A.A., Beitollahi, H., Zareyee, D., 2012. J. Mol. Liq. 168, 69–74.
Vasilescu, A., Andreescu, S., Bala, C., Litescu, S.C., Noguer, T., Marty, J.L., 2003. Biosens. Bioelectron. 18, 781–790.
Wang, C.Y., Wang, Z.X., Zhu, A.P., Hu, X.Y., 2006. Sensors 6, 1523–1536.
Wang, Y., Chen, Z.-Z., 2009. Colloids Surfaces B Biointerfaces 74, 322–327.
Yaghoubian, H., Beitollah, H., Soltani-Nejad, V., Mohadesi, A., Afzali, D., Zamani, H., Roodsaz, S., 2011. Int. J. Electrochem. Sci. 6, 1307–1316.
Yan, J., Wei, T., Fan, Z., Qian, W., Zhang, M., Shen, X., Wei, F., 2010b. J. Power Sources 195, 3041–3045.
Yan, J., Wei, T., Shao, B., Ma, F., Fan, Z., Zhang, M., Zheng, C., Shang, Y., Qian, W., Wei, F., 2010a. Carbon 48, 1731–1737.
Yu, Z., Li, X., Wang, X., Ma, X., Li, X., Cao, K., 2012. J. Chem. Sci. 124, 537–554.
Zhang, R., Jin, G.-D., Chen, D., Hu, X.-Y., 2009. Sens Actuators B:Chem. 138, 174–181.
Zhang, Y., Ren, W., Zhang, S., 2013. Int. J. Electrochem. Sci. 8, 6839–6850.
Zhao, Y., Zhao, S., Huang, J., Ye, F., 2011. Talanta 85, 2650–2654.